

Supporting information

1. Catalyst characterization techniques

To determine the information on the structural aspects of the catalyst including particle size and distribution as well as oxidation state of metal, the material was spectroscopically characterized after calcination using various techniques including Transmission electron microscopy (TEM), Fourier transformation infrared spectroscopy (FTIR) and X-ray photoelectron spectroscopy (XPS) before and after the reaction.

The TEM images of the material was recorded on Philips Technai operating at 200 Kv. The powder was suspended in ethanol by ultrasonic method. A drop of this solution was placed on a grid with a holey carbon copper film and then allowed to dry, covered by a watch glass. For FTIR, all the spectra were taken at room temperature on a Horiba spectrometer FT-720. Before measurement, samples were grounded with KBr and pressed into thin wafers. XPS spectra were recorded on an Ulvac PHI 5601ci spectrometer. All of the powder samples were fixed onto a copper sample holder using double-sided sticky tape, which was then placed into a vacuum chamber attached with a turbo molecular pump. The samples were outgassed for 1 day under vacuum (10^{-5} Pa) and then introduced into the analysis chamber, where the pressure was kept around 1×10^{-7} Pa. The pressure in the sample chamber was kept under 1×10^{-7} Pa. The binding energy scales were adjusted to the highest C (1s) peak position equal to 285 eV. To calculate the chemical composition of the samples, empirical sensitivity factors were obtained from the relative area intensities of the photoelectron spectra of compounds of known chemical composition. Monochromatized Al $K\alpha$ X-ray (14 kV, 200 W) was used in place of a conventional X-ray source to obtain high-quality spectra to avoid overlapping of the satellite peaks; thus, uncertainty in the determinations of the peak position and peak area was nullified. An electron flood gun was used as a neutralizer, and the number of acquisitions was maintained at 12 for each analysis. To ensure the accuracy of the data, the XPS system was calibrated using the peaks of Cu ($2P_{3/2}$) and Cu ($3P$) whose binding energies are 932.67 and 75.14 eV, respectively.

2. Method of product analysis

After the reaction, liquid product was separated from the solid catalyst by filtration and then subjected to identification using GC-MS (Varian CP3800). Quantitative analysis was carried out using a GC (HP 6890) equipped with HP-5MS capillary column (Agilent, 30 m x 0.32 mm, 0.25 μ m) and a flame ionization detector. The GC method used as follows: An initial oven temperature of 50 °C was held for 3 minutes. In the next step, the temperature was ramped at 10 °C/min. until it reached 100 °C and held at 100 °C for 2 minutes followed by the increase in temperature to 230 °C ramped at 7.5 °C/min. and held at 230 °C for 20 minutes. In this work, conversion and selectivity were calculated on carbon basis ^{1, 2}. Conversion of furfural is defined as moles of carbon in the furfural reacted (obtained from GC analysis) divided by the moles of carbon in furfural initially charged. The selectivity was calculated from the moles of product to the total moles of product x 100. Carbon balance was also checked, which remain constant of 95.5 \pm 2 %.

Reference

1. K. Chen, M. Tamura, Z. Yuan, Y. Nakagawa and K. Tomishige, *ChemSusChem* 2013, **6**, 613 .
2. J. Jae, W. Zheng, R. F. Lobo and D. G. Vlachos, *ChemSusChem* 2013, **6**, 1158.

3. Computational details

Calculation of adsorption energy: We have performed adsorption energy calculation using a Grand Canonical Monte Carlo (GCMC) method as implemented in Adsorption Locator software of Dassault Systemes Biovia. Possible adsorption configurations are identified by carrying out Monte Carlo searches of the configurational space of the substrate-adsorbate system as the temperature is slowly decreased according to a simulated annealing schedule ^{1, 2}. Here, we used a Pt (100) slab of 4 atomic layer thickness with a 12 layer of vacuum thickness. We have ensured the top layer as the targeted atoms. Each of the reactant and product molecules were allowed to adsorb within constrain of the periodicity at a constant

temperature of 80 °C (experimental temperature). Simulated annealing method is adopted as it is a metaheuristic algorithm for locating a good approximation to the global minimum of a given function in a large search space³. We obtain the adsorption energy for a mixture of the constituents with 1 molecule of the reactant/ product, 4 molecules of hydrogen in each case and added 32 molecules of CO₂ mimicking the condition of the reaction in CO₂. We have used COMPASS II (Condensed-phase Optimized Molecular Potentials for Atomistic Simulation Studies) force-field in the calculation as provided by Dassault Systemes BIOVIA⁴, that enables accurate and simultaneous prediction of gas-phase properties (structural, conformational, vibrational, and so on) and condensed-phase properties (equation of state, cohesive energies, and so on) for a broad range of organic and inorganic molecules^{5, 6}.

Method of activation energy calculation: Calculations have been performed using the DMol3 code of DASSAULT SYSTEMES BIOVIA^{7,8} with Perdew–Burke–Ernzerhof (PBE) exchange–correlation functional⁹. The Kohn–Shamequation was expanded in a double numeric quality basis set (DNP) with polarization functions. To consider the relativistic effect, the DFT Semi-core Pseudo-potentials¹⁰ are used for the treatment of the core electrons of the doped clusters. The orbital cut off range and Fermi smearing were selected as 5.0 Angstrom and 0.001 Ha respectively. The self-consistent-field (SCF) procedures were performed with the aim of obtaining well converged geometrical and electronic structures with a convergence criterion of 10⁻⁶ a.u. The energy, maximum force and maximum displacement convergence were set as 10⁻⁶ Ha, 0.002 Ha/ Å and 0.005/Å, respectively. Synchronous transit methods were employed to find the transition state followed by the construction of approximate minimum energy path through Nudged Elastic Band (NEB) method. After confirming the intrinsic reaction coordinate for the transition state, the vibration frequency for the single imaginary mode is confirmed. The rate coefficients are central to determining the rate of reaction. Often these coefficients are observed to have a strong dependence on temperature, T, which is usually expressed in an Arrhenius form or, more generally, a modified Arrhenius form:

$$k(T) = A \left(\frac{T}{T_0} \right)^n e^{-E_a/RT}$$

Where, A is referred to as the pre-exponential factor, T_0 is a reference temperature, R is the gas constant, E_a is the activation energy.

The Arrhenius expression is an empirical expression where the parameters A , n , and E_a are derived from experimental observation. $k(T)$ can also be estimated using transition state theory (TST). The Reaction energy barrier for Transition state is taken to calculate the parameters for Arrhenius equation including E_a and A . The model is chosen as 2 metal atom with 2 H in close vicinity of the metal atom with furfural and furfuryl alcohol as reactant and product itself, respectively (Figure S3).

References

1. V. Cerný, *J. Optim. Theor. Appl.*, 1985, **45**, 41-51.
2. D. Frenkel, B. Smit, *Understanding Molecular Simulation: From Algorithms to Applications*, 2nd Edition, Academic Press: San Diego, 2002.
3. S. Kirkpatrick, C. D. Gelatt, M. P. Vecchi, *Science* 220 (1983) 671-680.
4. H. Sun, Z. Jin, C. Yang, R. L. C. Akkermans, S. H. Robertson, N. A. Spensley, S. Miller, S. M. Todd, *J. Mol. Model.* 22 (2016)1.
5. H. Sun, *Macromolecules* 28 (1995) 701-712.
6. H. Sun, *Spectrochim. Acta Part A* 53 (1997)1301-1323.
7. B. Delley, *J. Chem. Phys.*, 1990, 92, 508–517.
8. B. Delley, *J. Chem. Phys.*, 2000, 113, 7756–7764.
9. J. P. Perdew, K. Burke and M. Ernzerhof, *Phys. Rev. Lett.*, 1996, 77, 3865–3868.
10. B. Delley, *Phys. Rev. B: Condens. Matter Mater. Phys.*, 2002, 66,155125.

Figure S1: Solubility of furfuryl alcohol in compressed CO₂. (a) furfuryl alcohol without CO₂ (b) after incorporation of 14 MPa of CO₂.

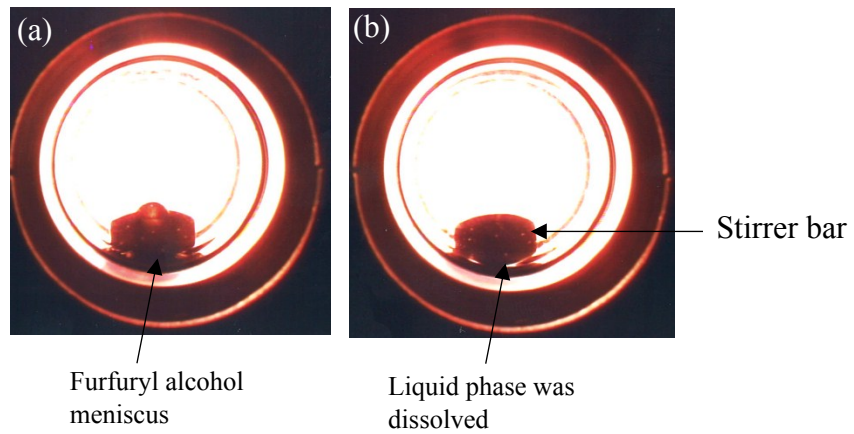


Figure S2: Change in phase behavior with fixed pressure and fixed density condition. At 35 °C (a) 8 MPa, (b) 6.4 MPa and at 100 °C (c) 8 MPa and (d) 8.7 MPa.

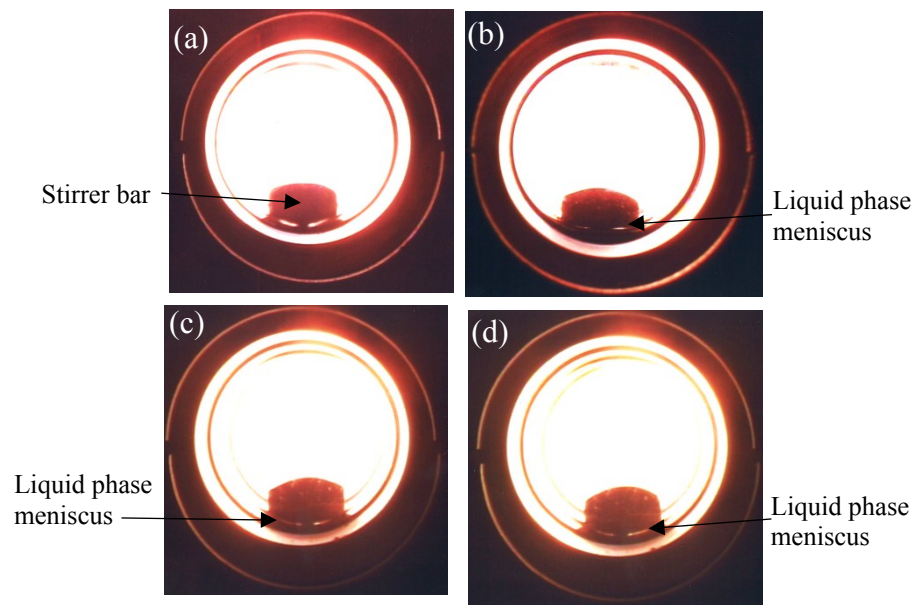


Figure S3: Model for activation energy calculations. Color code: blue= Pt, white= H, grey= C, red= O.

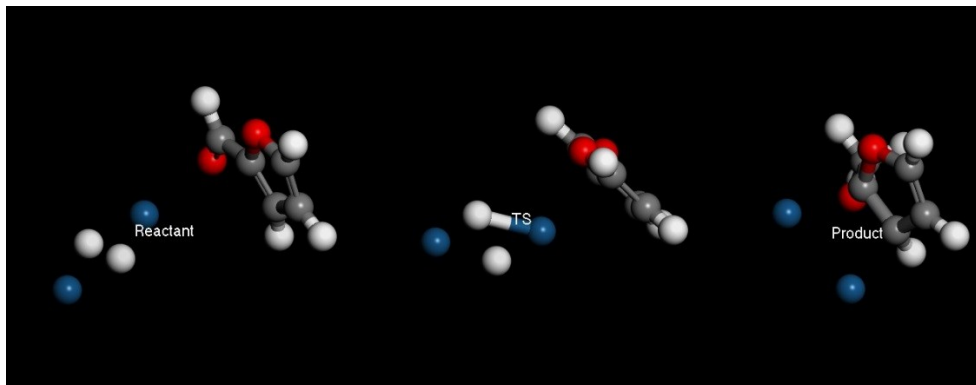


Figure S4: TEM image of the catalyst: (a) before reaction and after reaction in (b) compressed CO₂, (c) solvent-free condition. Average particle size = 5 ± 0.5 nm in each case.

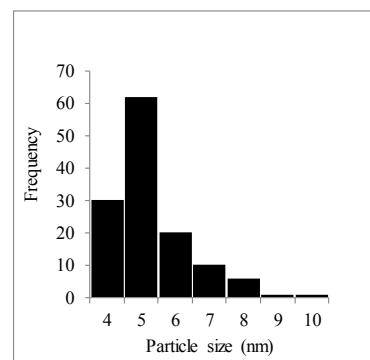
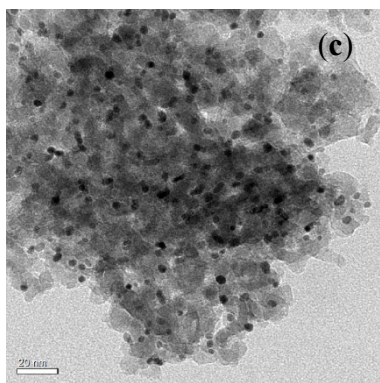
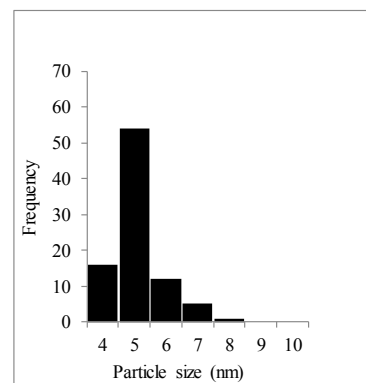
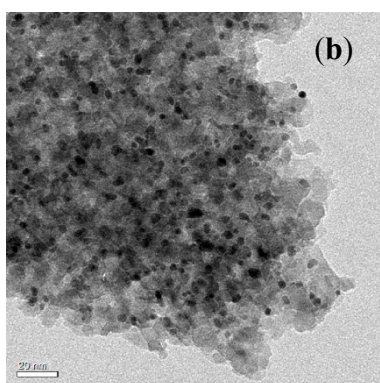
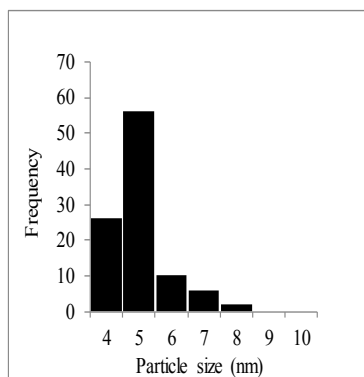
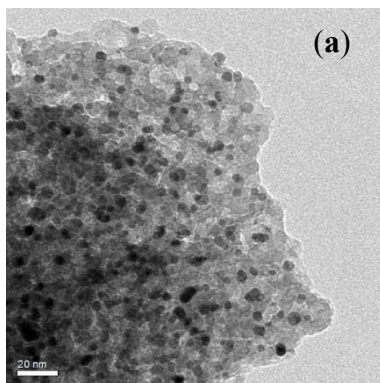


Figure S5: FTIR spectra of the catalyst: (a) before reaction and after reaction in (b) compressed CO₂, (c) solvent-free condition

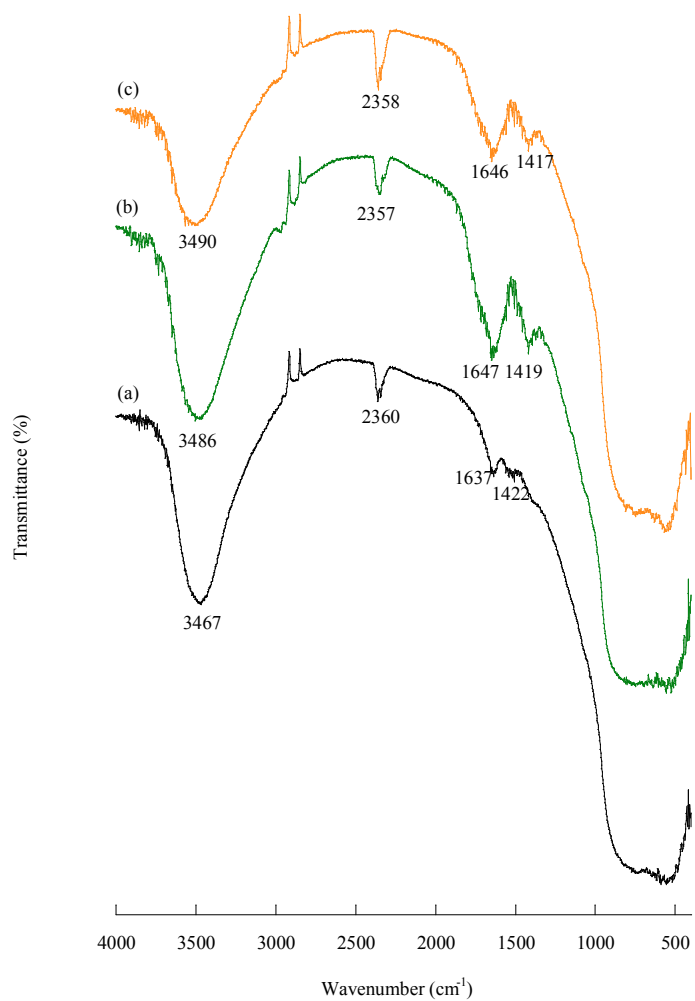


Figure S6: De-convoluted XPS spectra of Pt/Al₂O₃ representing Al 2p and Pt 4f: (a) before and after the reaction in (b) compressed CO₂, (c) solvent-less condition.

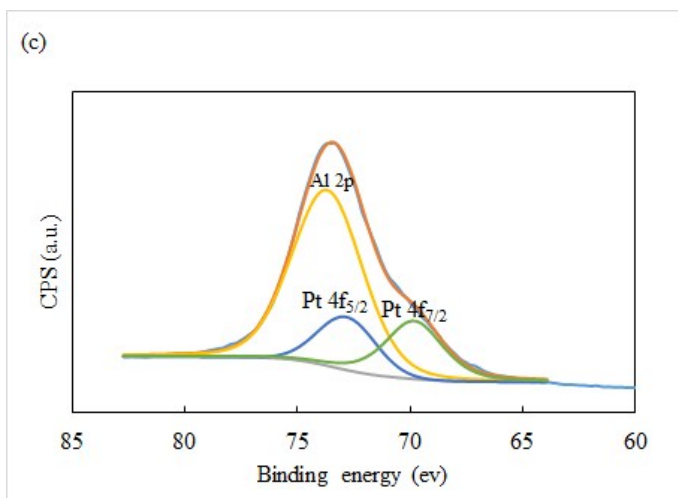
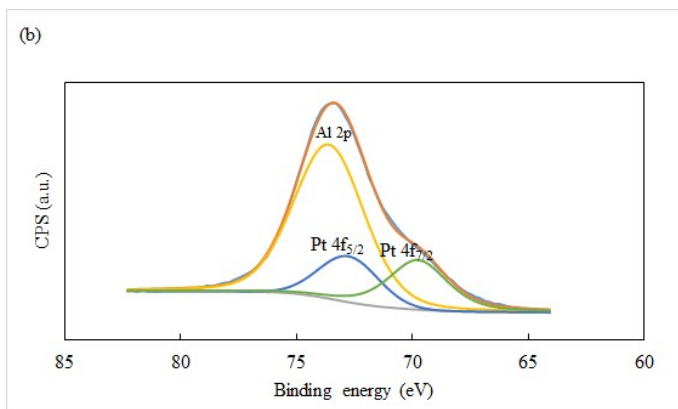
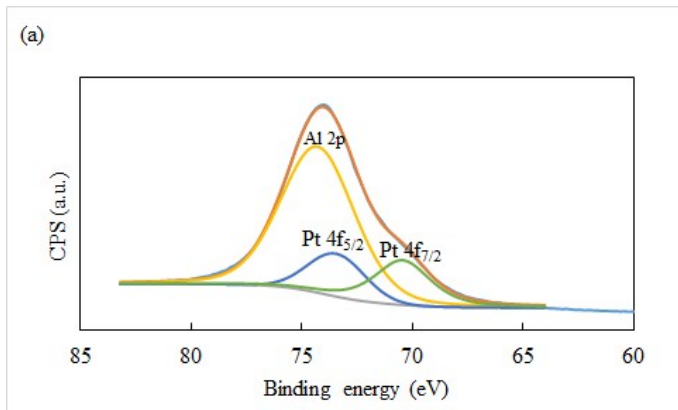


Figure S7: Recycling of Pt/Al₂O₃ catalyst

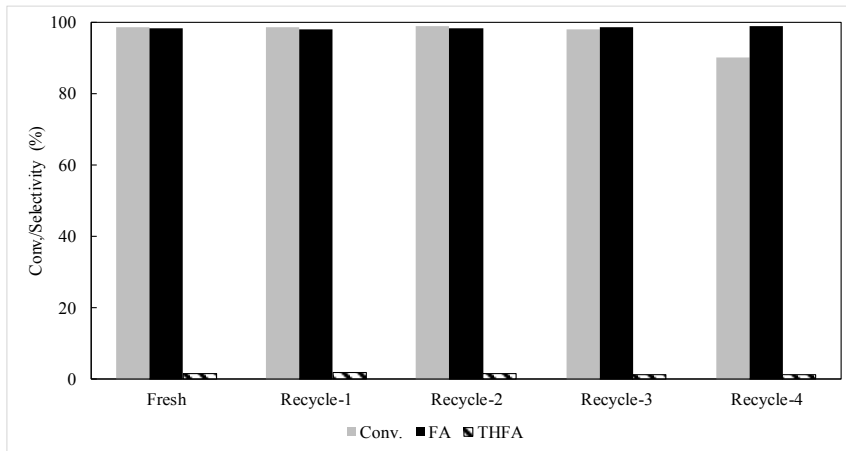


Table S1: Binding energies of C1s, O1s, Al 2p, Pt 4f_{7/2} and Pt 4f_{5/2} of fresh and used Pt/Al₂O₃ from compressed CO₂ and solvent-less condition. Surface composition is also presented.

Binding energy (eV)	Before reaction	After reaction	
		Compressed CO ₂	Solvent-less
O1s	530.0	530.3	530.5
Al 2p	74.4	73.7	73.7
Pt 4f _{7/2}	70.4	69.9	69.9
Pt 4f _{5/2}	73.4	72.4	72.5
Atomic concentration (%)			
O	54.9	54.9	56.5
Al	44.0	44.0	42.6
Pt	1.1	1.1	0.9